Rev. Mexicana Astron. Astrof., **22**, 243-248 (1991)

IMAGES AND LINE PROFILES FROM NONADIABATIC JET MODELS

A.C. Raga[1], S. Biro[2], J. Cantó[2], and L. Binette[1]

Received 1991 February 12

RESUMEN

El espectro de líneas de emisión de los objetos Herbig-Haro podría ser excitado por choques internos en un jet no adiabático. Exploramos esta posibilidad presentando predicciones de imágenes y diagramas posición-velocidad obtenidos mediante modelos de jets estacionarios y no adiabáticos. Por más que estos modelos predicen algunas de las características de los jets estelares, no logran reproducir en detalle los resultados observacionales. Este resultado parece sugerir que otros mecanismos de excitación podrían tambien ser importantes en los jets estelares.

ABSTRACT

The emission line spectrum observed in jet-like Herbig-Haro objects could be excited by internal "crossing shocks" in a nonadiabatic jet flow. We explore this possibility by presenting predictions of Hα and [S II] images and position-velocity diagrams (i.e., spatially resolved line profiles) from nonadiabatic, steady jet models. We find that while these models do predict some of the observed characteristics of stellar jets, they fail to reproduce in detail the observational results. This suggests that other excitation mechanisms might also be important in stellar jets.

Key words: **HERBIG-HARO OBJECTS – HYDRODYNAMICS**

I. INTRODUCTION

Dopita, Schwartz and Evans (1982) and Königl (1982) first suggested, from observational and theoretical (respectively) points of view, that some Herbig-Haro (HH) objects might be the result of a continuous, highly collimated outflow from a young star. Since then, a number of HH objects that are good candidates for this "stellar jet" interpretation have been discovered (see, e. g., Mundt and Fried 1983; Reipurth *et al.* 1986; Mundt, Brugel and Bührke 1987; Reipurth 1989a).

The prototype of the subclass of HH objects known as "stellar jets" is the HH 34 system (Reipurth *et al.* 1986; Bührke, Mundt and Ray 1988), which shows a chain of well aligned knots emanating from the source. At a distance of $\sim$ 30" from the source, this chain of knots disappears, and the emission reappears at $\sim$ 60" from the source in the object HH 34 (which is listed in the catalog of Herbig 1974). HH 34 has been interpreted as the working surface of the stellar jet.

We will concentrate on models for the production of well aligned chains of radiating knots, such as the one observed in HH 34. Other good examples of this type of structure are observed in HH 83 (Reipurth 1989a), HH 111 (Reipurth 1989b) and HH 30 (Mundt, Ray and Bührke 1988).

In the recent past (Raga, Binette and Cantó 1990), we have developed models of nonadiabatic, steady jets, in which the effects of nonequilibrium ionization and cooling are considered. These models represent a step forward with respect to the ionization equilibrium steady jet models of Falle, Innes and Wilson (1987), in that the more realistic treatment of the atomic processes which we are carrying out allow us to make more reliable predictions of observable parameters. Blondin, Fryxell and Königl (1990) have studied internal shocks in time-dependent (rather than steady) jets, but they have included only an approximate ionization equilibrium cooling function.

The results from steady, nonadiabatic jet models at this time appear to be in a rather firm theoretical footing. Apart from the numerical calculations of Falle *et al.* (1987) and Raga *et al.* (1990), an analytic theory for the formation of shocks in steady jets has been developed by Cantó, Raga and Binette (1989). Biro (1991) has carried out a detailed comparison between the analytic and numerical results.

1. Canadian Institute for Theoretical Astrophysics.
2. Instituto de Astronomía, UNAM.

However, comparisons between these theoretical models and observations of stellar jets are still at a very rudimentary state. In order to facilitate such comparisons between theory and observations, we present new predictions of observable quantities from the nonadiabatic, steady jet models of Raga *et al.* (1990). In particular, we discuss predictions of Hα and [S II] intensity maps and position-velocity diagrams. We then compare these predictions in a qualitative way with previously published observations of jet-like HH objects.

II. PREDICTIONS FROM NUMERICAL MODELS

We assume that we have an initially overpressured, steady, cylindrically symmetric jet immersed in a homogeneous, constant pressure environment The jet is also assumed to have an initial "top hat' cross section (i. e., at the injection point, the pressure, temperature and velocity of the flow are constant over the cross section of the jet). The characteristics of such a jet are determined by the initial jet radius r_0, hydrogen number density $n_{H,0}$, temperature T_0, jet to environment pressure ratio P_0/P_e and flow velocity v_0 (which we assume to be parallel to the symmetry axis). As discussed by Raga *et al.* (1990) and by Cantó *et al.* (1989) there are simple scaling laws that can be used to relate the properties of jets with different initial parameters. These authors also give a description of the equations, the numerical method, and the calculation of the non-equilibrium ionization radiative energy loss. The re-

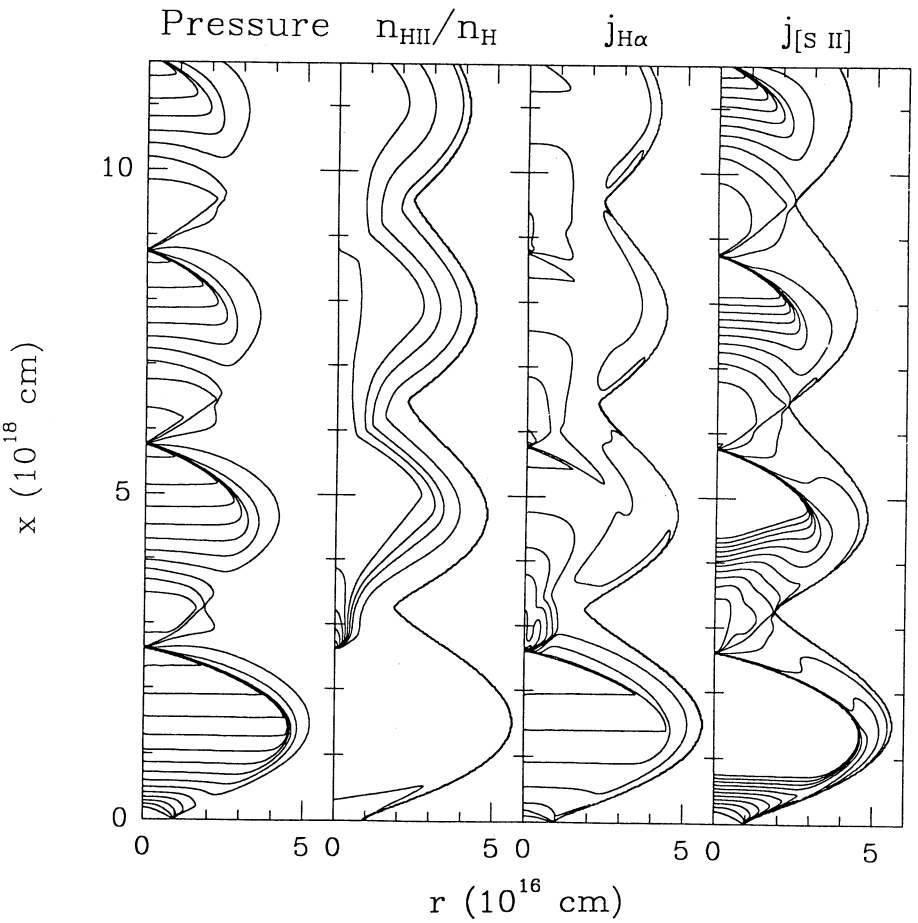

Fig. 1. From left to right: pressure stratification (succcessive contours represent factors of 2); hydrogen ionization fraction (successive contours represent factors of 2); Hα emission coefficient (successive contours represent factors of 10); and [S II] 6717+6731 emission coefficient (successive contours represent factors of 10) for the steady jet model discussed in the text. The initial ionization fraction of the jet (at $x = 0$) has a value of $\approx 3 \times 10^{-4}$ and the maximum ionization fraction (obtained right behind the first reflected shock, on the symmetry axis) has a value of ≈ 0.09, which illustrates the fact that only low ionization fractions are obtained.

sults presented in the present paper are calculated with a slightly modified version of the code by Raga *et al.* (1990), which is described by Biro 1991.

We will limit our discussion to one set of initial flow parameters : flow velocity $v_0 = 20$ km s^{-1}, jet radius $r_0 = 10^{16}$ cm, hydrogen number density $n_{H,0} = 10^4$ cm^{-3}, temperature $T_0 = 9000$ K, and jet to environment pressure ratio $P_0/P_e = 30$. Initially, the gas has an ionization fraction corresponding to coronal ionization equilibrium (i. e., collisional ionizations balanced by radiative and dielectronic recombinations) at the temperature T_0.

This assumption of initial coronal ionization equilibrium is quite arbitrary. For example, the gas injected into the jet flow could have an ionization fraction reflecting higher temperature and ionization conditions which might occur in the near environment of the source of the jet. We have computed models for different initial ionization fractions (not corresponding to coronal equilibrium at the initial temperature of the jet flow). These calculations show that for high initial ionization fractions, the emission from the region close to the injection point and the emission from the first crossing shock cell are stronger. However, the qualitative characteristics of the jet flow (and of the predicted intensity maps and line profiles) are not strongly affected by changes in the initial ionization fraction.

In Figure 1, we show the pressure, the hydrogen ionization fraction, and the Hα and [S II] 6717+31 emission coefficients as a function of position along and across the symmetry axis. The flow is divided into a number of "crossing shock cells", which are formed by incident/reflected shock pairs. From Figure 1, it is clear that the emission of each crossing shock cell is dominated by the emission from the post-reflected shock region (as has already been pointed out by Raga 1991). Also, we see that the Hα emission peaks (or "condensations", corresponding to each crossing shock cell) are spatially less extended than the [S II] condensations.

In Figures 2 and 3, we show the Hα and [S II] 6717+31 intensity maps and position-velocity diagrams predicted from our model. For the results shown in Figure 2, we have assumed that the flow is parallel to the plane of the sky; and in Figure 3, we have assumed an orientation angle of 45° (towards the observer) for the flow. The calculation of the position-velocity diagrams has been carried out by placing a "theoretical spectrograph slit" along the axis of the jet. The projection of the spectrograph slit on the plane of the sky is assumed to be wider than the jet diameter (so that all of the emission from the jet goes through the spectrograph slit).

The predicted images show a structure of aligned knots (or condensations), which correspond to the emission from the post-reflected shock region of the

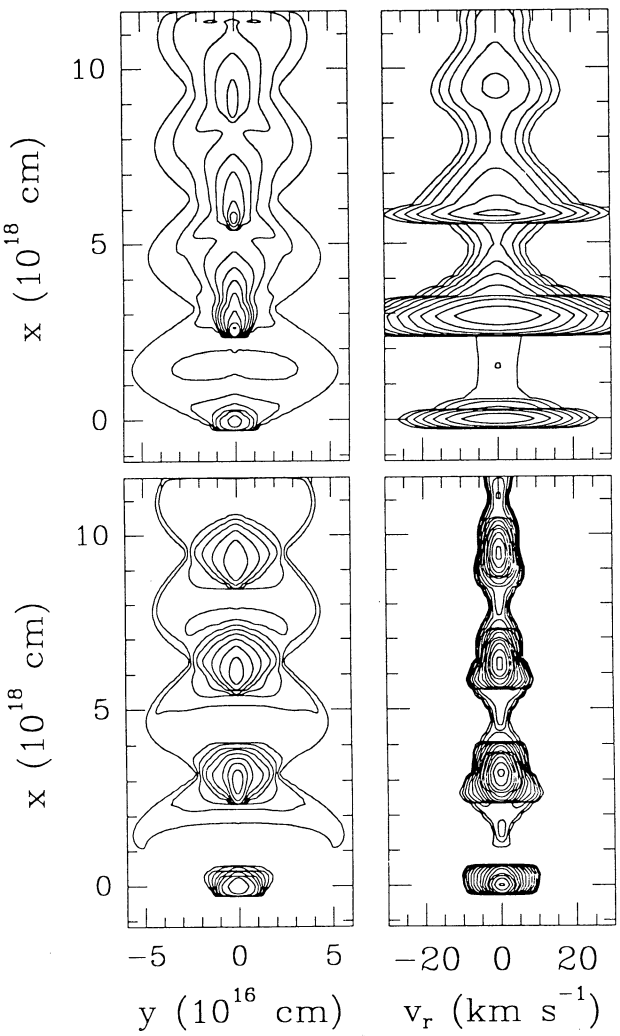

Fig. 2. Hα (top) and [S II] 6717+6731 (bottom) emission predicted from the jet model discussed in the text. The diagrams on the left are intensity maps (successive contours represent factors of 5), and the diagrams on the right are position-velocity diagrams (successive contours represent factors of 2). The flow is assumed to lie in the plane of the sky (see the text).

crossing shock cells (see Figures 2 and 3). The Hα knots are spatially more concentrated than the [S II] knots. The first crossing shock cell (the one closest to the source) produces the strongest emission, and the following ones are much fainter. For the two orientation angles shown in Figures 2 and 3 (0° and 45°, respectively), the only observed difference between the predicted intensity maps is a different scaling of the distance along the symmetry axis.

The predicted position-velocity diagrams also show the emission knots that result from the crossing shock cells (see Figure 2 and 3). For the case of a flow moving in the plane of the sky

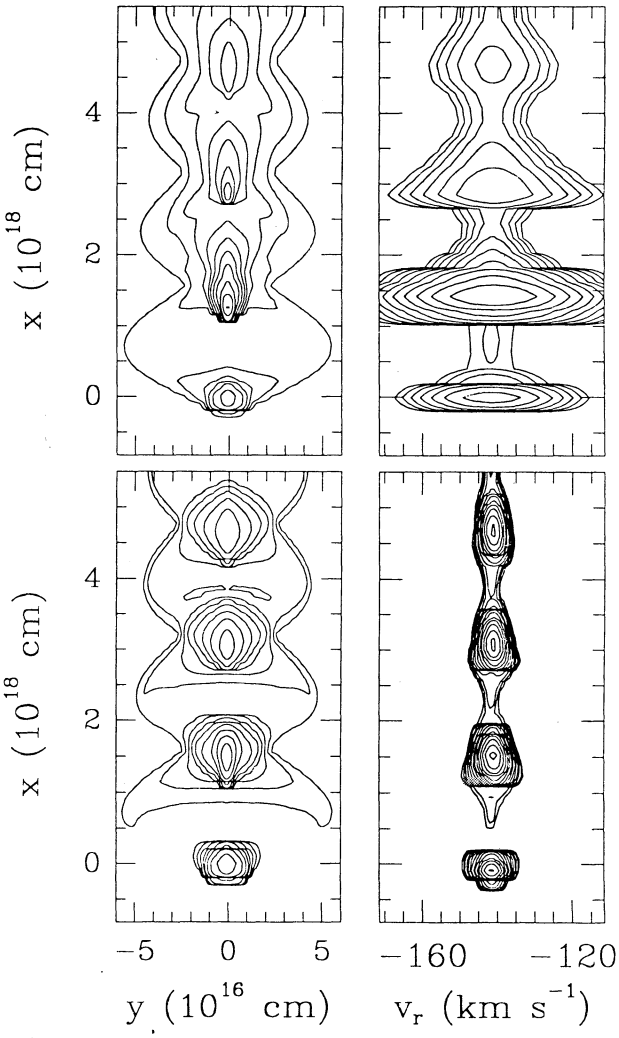

Fig. 3. Hα (top) and [S II] 6717+6731 (bottom) emission predicted from the jet model discussed in the text. The diagrams on the left are intensity maps (successive contours represent factors of 5), and the diagrams on the right are position-velocity diagrams (successive contours represent factors of 2). The jet is assumed to be flowing towards the observer, at an angle of 45° with respect to the plane of the sky (see the text).

(Figure 2), a very narrow line profile centered at zero velocity is observed. For a flow moving at 45° with respect to the plane of the sky (Figure 3), we see a narrow line profile centered at ≈ -141 km s^{-1} (which is the projection of the velocity of the jet along the line of sight) For both orientations of the flow, the line width is ~ 10-30 km s^{-1} (i. e., not much larger than the sound speed). The Hα line is broader than the [S II] line due to the difference between the thermal broadening of hydrogen and sulphur.

The absence of more interesting effects in the position-velocity diagrams is a direct result of the fact that the internal shocks in the jet flow are very oblique (this effect is discussed in detail by Cantó *et al.* (1989). Because of this, the velocity of the flow is always closely parallel to the symmetry axis (the velocities perpendicular to the axis are comparable to the sound speed), resulting in the production of very narrow line profiles.

III. DISCUSSION

In this paper, we have discussed predictions of observable quantities from the steady jet model developed by Raga *et al.* (1990) and Biro (1991). In this model, a realistic treatment of the non-equilibrium cooling is made, allowing us to obtain more or less reliable predictions of the spatial distribution of the emission. Other recent models of stellar jets (Falle *et al.* 1987; Raga 1988; Blondin, Königl and Fryxell 1989; Tenorio-Tagle 1989) have been calculated with simplified cooling functions computed either for coronal ionization equilibrium or for an isobaric, undisturbed parcel cooling from high temperatures. Both of these assumptions are incorrect for the case of stellar jets, where parcels go through a series of shocks, and also through compression and expansion regions.

Even though these simplified cooling functions would result in unreliable predictions of emission line strengths, they apparently are adequate for qualitatively reproducing the effects on the flow of the radiative cooling. We find that our fully non-equilibrium ionization steady jet models produce shock patterns that are in good agreement with the calculations of Falle *et al.* (1987, who used an isobaric cooling function, as described above). From this, we conclude that the introduction of a more realistic treatment of the radiative cooling does not strongly affect the qualitative characteristics of the flow.

We have presented the Hα and [S II] intensity maps and position-velocity diagrams predicted from a steady, non-adiabatic jet model. We find that the predicted intensity maps show a series of aligned intensity maxima, which correspond to the post-reflected shock regions of the crossing shock cells.

Although this condensation structure does agree in a qualitative way with narrow band images of jet-like HH objects, the knot separation to knot width ratios l_{knot}/D_{knot} do not seem to be in agreement with observations of the well studied HH 34 jet (see, e. g., Reipurth *et al.* 1986; Raga and Mateo 1988; Bührke *et al.* 1988). While for the knots of HH 34 one obtains $l_{knot}/D_{knot} \approx 2$, the corresponding value from crossing shock models is $l_{knot}/D_{knot} \sim 1.4 \times M_j$ (see Raga 1989), where $M_j \sim 20$ is the Mach number of the jet.

This theoretical l_{knot}/D_{knot} ratio corresponds to the ratio of the knot separation to the maximum diameter of the crossing shock cells. However, our predicted intensity maps show that the observed diameter of the emitting region can be substantially smaller (see Figures 2 and 3). Furthermore, the knots of the HH 34 jet show large proper motions along the symmetry axis (Reipurth 1989c), also in clear disagreement with the interpretation of these emission knots as crossing shock cells in a steady jet.

We should note that the time-dependent numerical simulations of Blondin *et al.* (1990) show some effects that might be in better agreement with the observations of the HH 34 jet. In these simulations, the head of the jet leaves a disturbed "wake" (possibly produced by the shedding of vortices) that surrounds the beam of the jet. The disturbances in this wake excite time-dependent crossing shocks in the jet flow. These crossing shock cells move along the jet with a proper motion $\sim 1/2$ of the velocity of the flow, and have knot separation to knot width ratios $l_{knot}/D_{knot} \sim 2-3$. Both the high proper motion and the l_{knot}/D_{knot} values are in good agreement with the observations of HH 34 mentioned above. Blondin *et al.* (1990) mention that these crossing shocks have normal shock velocities ~ 30 km s^{-1} in their $v_0 = 200$ km s^{-1} jet simulation. From this, one would conclude that the emission line profiles resulting from this flow would have line widths similar to the ones obtained from our steady jet models.

However, as has been noted by Tenorio-Tagle (1989), the time-dependent crossing shocks described above only appear close to the head of the jet, and only one or two crossing shock cells are observed at any given time. This is also clearly seen in the numerical calculations of Blondin *et al.* (1990). This result does not agree with the observations of most stellar jets (including HH 34), which show a number of aligned knots close to the source, and then an extended "gap" with no emission between these knots and the head of the jet. Because of this, we conclude that even though the time-dependent crossing shocks described by Blondin *et al.* (1990) do reproduce the observed length to width ratios and proper motions of the knots of HH 34, they apparently fail to explain the general morphology of this jet. Conversely, while the steady jet models can explain the general morphology of stellar jets (with bright knots close to the source, followed by a gap with no emission separating the knots from the head of the jet), they fail to explain the length to width ratios and the proper motions of the jet knots.

At this time it is not clear whether or not the condensation structures of other jet-like HH objects can be more successfully interpreted in terms of steady jet models. For example, the HH 30 jet (Mundt *et al.* 1988; Mundt *et al.* 1990) shows a structure of better separated knots, with l_{knot}/D_{knot} values $\sim 10-15$, which are in much better agreement with the predictions from steady jet models.

The position-velocity diagrams predicted from our steady jet model show very narrow line profiles (with widths $\sim 10-30$ km s^{-1}) centered at a velocity that corresponds to the projection along the line of sight of the jet velocity. This is to a certain extent in qualitative agreement with observations of jet-like HH objects, which in many cases do show narrow emission line profiles. However, the changes in radial velocity as a function of position along the flow axis that have been observed for some stellar jets (see, e. g., Reipurth 1989a, b, c; Solf and Böhm 1991) are not reproduced by our steady jet models. Also, the extended, low velocity wings which are sometimes observed (in addition to the narrow emission component at the projection of the jet velocity) in jet-like HH objects is not explained by our models. Solf (1987), and Meaburn and Dyson (1987) have suggested that this emission might arise in a turbulent mixing layer at the outer boundary of the jet flow.

We conclude by noting the following. The models that we have presented have serious limitations, to a large extent because time-dependent effects (which seem to be important in stellar outflows) have not been considered. However, at this time these models are the only available calculations of axisymmetric, nonadiabatic jet flows with a realistic treatment of the relevant atomic processes. Because of this, the models that we have presented provide a unique opportunity for a possible comparison of the emission line spectrum of jet-like HH objects with theoretical predictions.

We acknowledge the very helpful and relevant comments made by the (anonymous) referee. The work of A.R. and L.B. was supported by the Natural Sciences and Engineering Research Council of Canada. The work of S.B. and J.C. has been partially supported by the DGAPA (UNAM) grant number IN-01-05-89. A.R. would like to thank Bo Reipurth and Jorge Melnick for making possible a visit to ESO (La Silla), during which part of this work was carried out.

REFERENCES

Biro, S. 1991, B. Sc. Thesis (Universidad Nacional Autónoma de México).

Blondin, J.M., Königl, A., and Fryxell, B.A. 1989, *Ap. J.*, (*Letters*) **337**, 37.

Blondin, J.M., Fryxell, B.A., and Königl, A. 1990, *Ap. J.*, **360**, 370.

Bührke, T., Mundt, R., and Ray, T.P. 1988, *Astr. and Ap.*, **200**, 99.

Cantó, J., Raga, A.C., and Binette, L. 1989, *Rev. Mexicana Astron. Astrof.*, **17**, 65.
Dopita, M.A., Schwartz, R.D., and Evans, I. 1982, *Ap. J. (Letters)*, **263**, L73.
Falle, S.A.E.G., Innes, D.E., and Wilson, M.J. 1987, *M.N.R.A.S.*, **225**, 741.
Herbig, G. 1974, *Lick Obs. Bull.*, No. 658.
Königl, A. 1982, *Ap. J.*, **261**, 115.
Meaburn, J., and Dyson, J.E. 1987, *M.N.R.A.S.*, **225**, 863.
Mundt, R., Brugel, E.W., and Bührke, T. 1987, *Ap. J.*, **319**, 275.
Mundt, R., and Fried, J.W. 1983, *Ap. J. (Letters)*, **274**, L83.
Mundt, R., Ray, T.P., and Bührke, T. 1988, *Ap. J. (Letters)*, **333**, L69.
Mundt, R., Ray, T.P., Bührke, T., Raga, A.C., and Solf, J. 1990, *Astr. and Ap.*, **232**, 37.
Raga, A.C. 1988, *Ap. J.*, **335**, 820.
Raga, A.C. 1989, in ESO workshop on *Low Mass Star Formation and Pre-Main Sequence Objects*, ed. B. Reipurth (Garching: ESO), p. 281.
Raga, A.C. 1991, *A.J.*, **101**, 1472.
Raga, A.C., Binette, L., and Cantó, J. 1990, *Ap. J.*, **360**, 612.
Raga, A.C., and Mateo, M. 1988, *A.J.*, **95**, 543.
Reipurth, B. 1989a, *Astr. and Ap.*, **220**, 249.
Reipurth, B. 1989b, *Nature*, **340**, 42.
Reipurth, B. 1989c, in ESO workshop on *Low Mass Star Formation and Pre-Main Sequence Objects*, ed. B. Reipurth (Garching: ESO), p. 247.
Reipurth, B., Bally, J., Graham, J.A., Lane, A.P., and Zealey, W.J. 1986, *Astr. and Ap.*, **164**, 51.
Solf, J. 1987, *Astr. and Ap.*, **184**, 322.
Solf, J., and Böhm, K.H. 1991, *Ap. J.*, **375**, 618.
Tenorio-Tagle, G. 1989, in *Structure and Dynamics of the Interstellar Medium*, eds. G. Tenorio-Tagle, M. Moles and J. Melnick (Berlin: Springer-Verlag), p. 264.

L. Binette and A.C. Raga: Canadian Institute for Theoretical Astrophysics, 60 St. George Street, Toronto, Ontario M5S 1A1 Canada.
S. Biro and J. Cantó: Instituto de Astronomía, UNAM, Apartado Postal 70-264, 04510 México, D.F., México.